A second-order adaptive sharp-interface method for incompressible multiphase flow

M. Sussman[1], M.Y. Hussaini[2], K. M. Smith[2], Ren Zhi-Wei[1], and V. Mihalef[3]

[1] Department of Mathematics, Florida State University, Tallahassee, FL 32306
[2] School of Computational Science and Information Technology, Florida State University, Tallahassee, FL 32306
[3] CBIM, Rutgers, The State University of New Jersey, Piscataway, NJ 08854

Abstract

The present method combines the advantages of the Cartesian-grid approach, second-order coupled level set and volume-of-fluid approach, and the dynamic adaptive mesh refinement(AMR) procedure to treat complex three-dimensional problems with sharp interfaces. Its accuracy and robustness are demonstrated by its application to bubble dynamics, ship hydrodynamics, and "water crown" computation. It is shown to capture or preserve sharp slip-lines, phase boundaries remarkably well.

1 Introduction

Discretization strategies for the treatment of problems containing slip-lines and phase boundaries in incompressible flow generally fall into the following distinct categories: continuum approach including level set and volume-of-fluid methods(e.g., Brackbill, et al. [3, 12, 11]), Cartesian-grid approach (e.g., Ye, et al. [13]) and ghost fluid or"dummy cell" method (e.g., Nguyen, et al. [6]; Helenbrook, et al. [5]). The continuum approach is robust and formally second-order accurate. However, it can excessively smear jumps in tangential velocity and its overall accuracy is affected by the low-order treatment of moving boundary conditions (see e.g., [9]). In the work of Nguyen, et al., the convergence of the interface location is first-order accurate that will consequently affect the overall accuracy of the method. Ye, et al. [13] employ front-tracking on a two-dimensional Cartesian grid, and it is not clear if the method can handle complex three-dimensional geometries with large density ratios. Helenbrook, et al. [5] developed a second-order method for two-phase flows, but the applications did not include complex geometries. It is unlikely that a straightforward application of their methods is possible to flow configurations with such wide parameter ranges and complex geometries as in the present study. The present effort develops an accurate and robust methodology that employs semi-implicit Crank-Nicolson temporal discretization and a spatial discretization strategy based on the second-order coupled level set and volume-of-fluid approach, the Cartesian-grid approach, and dynamic adaptive mesh refinement. The present methodology retains the advantages of these methods while precluding their weaknesses.

2 Governing Equations and Solution Technique

The governing equations are the well-known three-dimensional incompressible unsteady Navier-Stokes equations for multiphase flows with appropriate jump relations at interface boundaries [4]. The solution technique is described below on a single uniform rectangular mesh. Details on the extension to an adaptive hierarchy of rectangular grids are given in [8]. Simply stated, adaptive grids are dynamically added and deleted over the course of a simulation depending on resolution requirements, and in the present computations, they cluster near the interface between fluids.

The variables for the two fluids are computed and stored *separately*, and then the solutions in the two fluids are coupled during the implicit computation of the new pressure and the viscous forces. Figure 1 illustrates the locations of the discrete variables. We provide here a brief outline of the method.

1. Advance the location of the interface using the coupled level set and volume-of-fluid method ([9, 7]).
2. Calculate nonlinear advective force terms in each fluid *separately* using high order, upwind, slope limited discretization.
3. Implicit Crank-Nicolson computation of viscous forces [1]. The new velocity field is continuous across the phase boundary (zero level set). Surface tension is included as a body force as in [9] except with zero thickness. Curvature is calculated directly from the volume fractions as described in [7].
4. Implicit calculation of updated pressure and solenoidal velocity field (projection step):

$$\nabla \cdot \frac{\nabla p}{\rho} = \nabla \cdot \boldsymbol{V} \qquad \boldsymbol{u} = \boldsymbol{V} - \frac{\nabla p}{\rho} \tag{1}$$

   The new velocity field satisfies the continuity condition and the new pressure satisfies the appropriate jump relations. The Cartesian-grid approach is used to approximate the divergence operator. We resort to an additional "correction" pressure solve to accurately enforce the continuity condition at the phase interface. The resulting matrix systems are symmetric and are solved by the multigrid preconditioned conjugate gradient method.
5. Extend liquid variables into the gas, and extend gas variables into the liquid (see [7]).

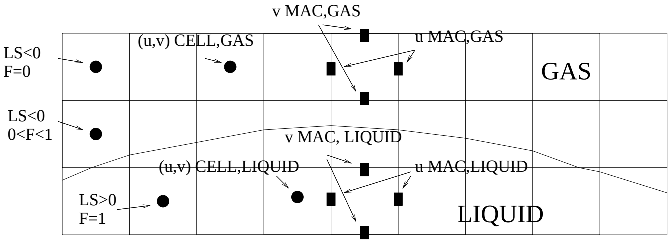

Fig. 1. Location of level set function, LS, volume-of-fluid function F, MAC velocity $\boldsymbol{U}^{MAC}$ and CELL velocity $\boldsymbol{U}^{CELL}$ in relation to the computational grid.

3 Results

3.1 bubble dynamics

We present two examples. For the first example, the density ratio is 1000:1, viscosity is zero, and the surface tension coefficient is 1/200. For the second example, the density ratio is 1050:1, the viscosity ratio is 31765:1, the liquid viscosity is 0.54 and the surface tension coefficient is 0.078. Results for the inviscid bubble are found to be similar to those of [10] which were obtained by the boundary integral method and "continuum" approach. Comparison of the results for the viscous bubble with the experimental observations of Bhaga and Weber[2] indicate good agreement (not shown owing to limited space).

The rate of convergence of the present method (Figure 2) is studied by refining the grid by a factor of two, and checking the difference or error between the level set function values on the coarse- and fine-grids. The error is defined as

$$E = \frac{\sum_{\Gamma_{ij}} |\phi^c_{ij} - \phi^f_{ij}|}{\sum_{\Gamma_{ij}} 1}, \qquad \Gamma_{ij} = \left\{(i,j) | \phi^c_{ij} \mathrm{or} \phi^f_{ij} \mathrm{changes\ sign}\right\}$$

where ϕ^c and ϕ^f correspond to the coarse-grid and fine-grid level set functions respectively. The error for varying grid resolutions is given in Table 1, which clearly demonstrates second-order convergence.

Table 1. Grid refinement study; left: inviscid air bubble rising in liquid, $t = 1.25$, $r = 1$; right: viscous air bubble rising in liquid, $t = 0.25$, $r = 0.013$.

coarse grid size	fine grid size	E
32x64	64x128	0.0102
64x128	128x256	0.0028

coarse grid size	fine grid size	E
32x64	64x128	0.00069
64x128	128x256	0.00017

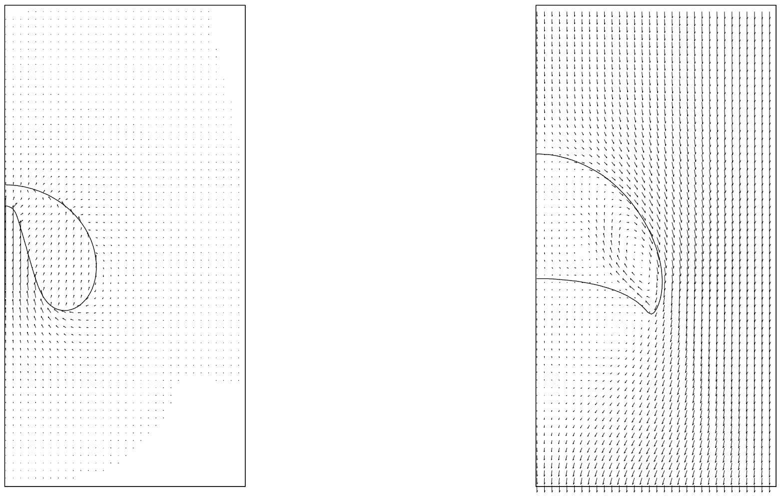

Fig. 2. Axisymmetric gas bubbles rising in a liquid medium; 128x256 grid; left: inviscid bubble, right: viscous bubble.

3.2 Three-dimensional ship hydrodynamics

Figure 3 shows wave overturning at the bow of a DDG5415 navy ship (details of ship geometry provided at http://www50.dt.navy.mil/5415/). The density ratio of water to air is 1000:1. The ship runs lengthwise from $x = 0.0$ to $x = -1.0$. Figure 4 compares the numerical predictions (continuous line) of wave height above the quiescent level with the whisker-probe measurements (jagged line) at various positions along the x-axis. In general, the agreement between predictions and measurements is very good. Table 2 presents the details of adaptive mesh refinement: the first column gives the number of levels of refinement, the second column the number of grid blocks together with the number of blocks added at each refinement level, the third column the total number of cells, the fourth column the number of processors, the fifth column the minimum mesh width and the last column the cpu time in seconds per timestep. The speed-up due to increasing the processors or the levels of adaptivity is found to slightly exceed 70%.

3.3 Three-dimensional "water crown" computation

Figure 5 illustrates a spherical water drop falling on the surface of water and the consequent formation of what is known as "water-crown". The present method sharply captures the evolution of the fluid interface merging and breaking on a relatively coarse mesh of dimensions 32x32x64.

Table 2. CPU time per time step for varying levels of adaptivity; 3D ship hydrodynamics.

levels	grids	cells	δ	processors	CPU time/step
1	64	2097152	1/128	32	376
2	64+148	5324800	1/256	32	1300
3	64+116+475	17940480	1/512	64	3000

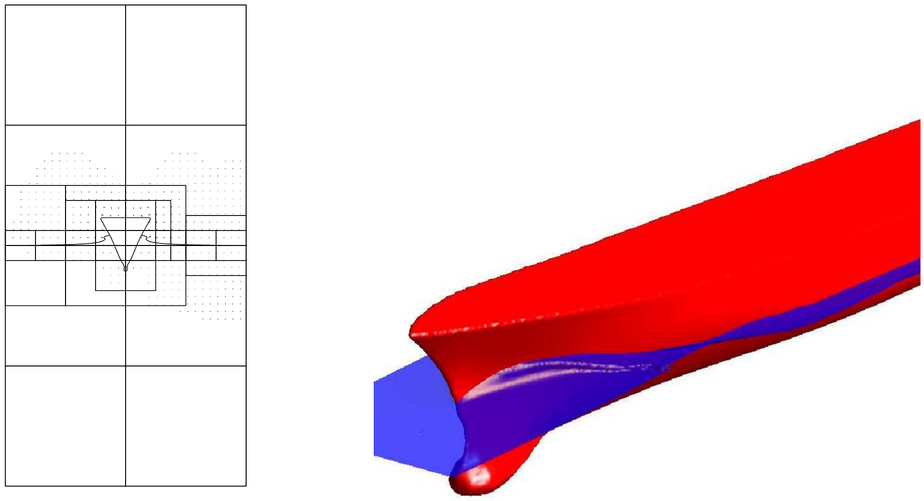

Fig. 3. Left: AMR grid for DDG5415 at $x = -0.1$; right: bow view of DDG5415.

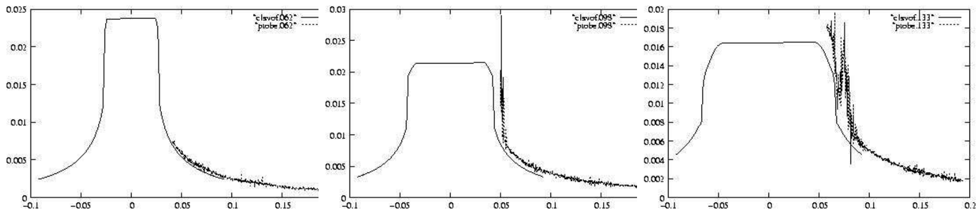

Fig. 4. Wave height predictions compared to whisker-probe measurements for the DDG5415; left to right: $x = -0.062$, $x = -0.098$, $x = -0.133$.

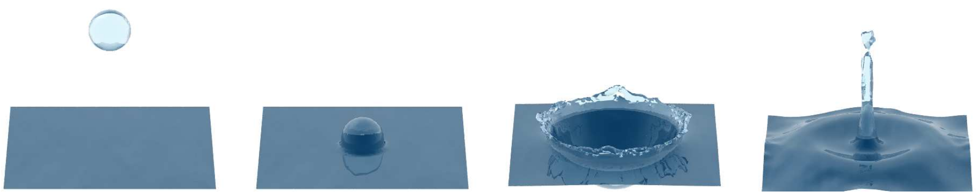

Fig. 5. "Water crown" computation; 32x32x64 grid

4 Conclusions

The accuracy and efficiency of the present method is demonstrated by the solutions to the problems of bubble dynamics, ship hydrodynamics and the "water crown." These computational tests indicate that the results previously obtained on fine meshes can now be obtained on a relatively coarse mesh, resulting in a speed-up of 8:1. We also show that additional speed-up results from the use of adaptive mesh refinement and parallelization. Evidently, the present method robustly handles the merging and breaking of fluid interfaces involving density ratios on the order of 1000:1.

References

1. J. B. Bell, P. Colella, and H. M. Glaz. A second-order projection method for viscous, incompressible flow. In *8th AIAA Computational Fluid Dynamics Conference*, Honolulu, June 9–11, 1987.
2. D. Bhaga and M.E. Weber. Bubbles in viscous liquids: Shapes, wakes and velocities. *J. Fluid Mech.*, 105:61–85, 1981.
3. J. U. Brackbill, D. B. Kothe, and C. Zemach. A continuum method for modeling surface tension. *J. Comput. Phys.*, 100:335–353, 1992.
4. Y.C. Chang, T.Y. Hou, B. Merriman, and S. Osher. Eulerian capturing methods based on a level set formulation for incompressible fluid interfaces. *J. Comput. Phys.*, 124:449–464, 1996.
5. B. Helenbrook, L. Martinelli, and C. Law. A numerical method for solving incompressible flow problems with a surface of discontinuity. *Journal of Computational Physics*, 148:366–396, 1999.
6. D. Nguyen, R. Fedkiw, and M. Kang. A boundary condition capturing method for incompressible flame discontinuities. *J. Comput. Phys.*, 172:71–98, 2001.
7. M. Sussman. A second order coupled levelset and volume of fluid method for computing growth and collapse of vapor bubbles. *Journal of Computational Physics*, 187:110–136, 2003.
8. M. Sussman. A parallelized, adaptive algorithm for multiphase flows in general geometries. *International Journal of Computers and Structures*, 2004. to appear.
9. M. Sussman and E.G. Puckett. A coupled level set and volume of fluid method for computing 3d and axisymmetric incompressible two-phase flows. *J. Comp. Phys.*, 162:301–337, 2000.
10. M. Sussman and P. Smereka. Axisymmetric free boundary problems. *J. Fluid Mech.*, 341:269–294, 1997.
11. M. Sussman, P. Smereka, and S.J. Osher. A level set approach for computing solutions to incompressible two-phase flow. *J. Comput. Phys.*, 114:146–159, 1994.
12. S. O. Unverdi and G. Tryggvason. A front-tracking method for viscous, incompressible, multi-fluid flows. *J. Comput. Phys.*, 100:25–37, 1992.
13. T. Ye, W. Shyy, and J.N. Chung. A fixed-grid, sharp interface method for bubble dynamics and phase change. *J. Comp. Phys.*, 174:781–815, 2001.